Observation of coherent destruction of tunneling and unusual beam dynamics due to negative coupling in three-dimensional photonic lattices

Peng Zhang,[1] Nikolaos K. Efremidis,[2] Alexandra Miller,[1] Yi Hu,[1,3] and Zhigang Chen[1,3,*]

[1]*Department of Physics and Astronomy, San Francisco State University, San Francisco, California 94132, USA*

[2]*Department of Applied Mathematics, University of Crete, Crete, Greece*

[3]*The Key Laboratory of Weak-Light Nonlinear Photonics, Ministry of Education and TEDA Applied Physics School, Nankai University, Tianjin 300457, China*

**Corresponding author: zhigang@sfsu.edu*

Received July 20, 2010; accepted August 19, 2010;
posted September 7, 2010 (Doc. ID 131868); published September 24, 2010

We demonstrate coherent destruction of tunneling (CDT) in optically induced three-dimensional photonic lattices. By fine-tuning the lattice modulation, we show unusual behavior of beam propagation, including light tunneling inhibition, anomalous diffraction, and negative refraction mediated by zero or negative coupling in the waveguide arrays. Image transmission based on CDT is also proposed and demonstrated. Our experimental results are in good agreement with our theoretical analyses.

OCIS codes: 160.5293, 190.4420, 130.2790.

Wave propagation in periodic structures occurs in many branches of physics. In optics, photonic lattices have served as a test bench for studying both linear and nonlinear wave phenomena in discrete systems [1,2]. It has been shown that longitudinal modulation in one- or two-dimensional (2D) lattices provides additional possibilities for control of beam propagation, even in the linear regime. For example, diffraction management [3], inhibition of light tunneling [4,5], multicolor dynamic localization [6], Rabi oscillation [7], and negative coupling [8] have been proposed and demonstrated in longitudinally modulated or curved waveguide arrays. Much richer phenomena are expected in three-dimensional (3D) photonic lattices [9–11], but their experimental demonstration remains a challenge owing to the difficulties in fabricating the desired 3D lattice structures. Recently, 3D photonic lattices have been created with the optical induction technique [12,13]. In this Letter, we demonstrate optical control of beam propagation dynamics in 3D photonic lattices. By using lattice superposition, we propose a way of optical induction of 3D photonic structures in bulk nonlinear materials. Inhibition of light tunneling, or better known as coherent destruction of tunneling (CDT), in two transverse dimensions is first demonstrated. In addition to CDT-based image transmission, anomalous diffraction and negative refraction resulting from negative coupling in the waveguide arrays are also proposed and demonstrated. Our experimental results are corroborated with theoretical and numerical analyses.

Propagation of an optical beam in a 3D photonic lattice optically induced in a biased photorefractive crystal can be described by the following Schrödinger equation:

$$\left(\frac{\partial}{\partial z}-\frac{i}{2}\nabla^2\right)u(\vec{r})=i[I_l/(1+I_l)]u(\vec{r}), \tag{1}$$

where $\nabla^2=\partial^2/\partial x^2+\partial^2/\partial y^2$ is the term determining transverse diffraction, $u(\vec{r})$ is the amplitude of the probe beam, and I_l is the intensity of the lattice-inducing beam. To induce a 3D photonic lattice with out-of-phase index modulation along the z direction among the adjacent waveguides [5,9,11], we choose $I_l=(2+A\cos Kz)\cos^2(\pi x/\Lambda)\cos^2(\pi y/\Lambda)+(2-A\cos Kz)\sin^2(\pi x/\Lambda)\sin^2(\pi y/\Lambda)$, where Λ is the transverse lattice spacing and A and K determine the normalized amplitude and the modulation frequency along the z direction, respectively, as shown in Fig. 1. To analyze the beam dynamics in our optically induced 3D lattice, let us start with a model from the coupled-mode theory:

$$i\frac{du_{m,n}}{dz}+C(u_{m+1,n}+u_{m-1,n}+u_{m,n+1}+u_{m,n-1})+\frac{A}{2}(-1)^{m+n}\cos(Kz)u_{m,n}=0, \tag{2}$$

where C is the coupling coefficient between adjacent waveguides. Using the asymptotic analysis [5,9,14], we obtain the effective (or average) coupling coefficient as $\bar{C}=KJ_0(A/K)$. In addition, by numerically employing Floquet theory [14], the coefficient $\bar{C}$ is computed from the quasi-energy band edges. Figure 1(c) depicts typical numerical (shaded areas) and analytical (dashed curve) results, which show that the coupling coefficient

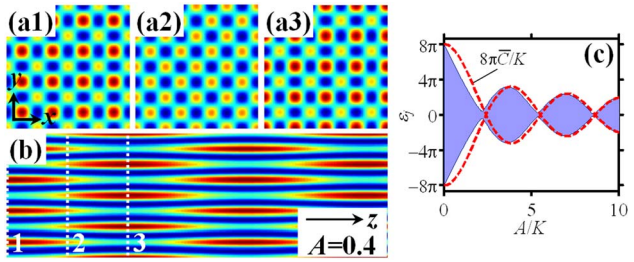

Fig. 1. (Color online) (a) Intensity patterns of the lattice-inducing beam at different transverse (x–y) planes marked by dashed lines in (b) side view (y–z) of the lattice beam propagating along the longitudinal z direction when the amplitude of modulation $A=0.4$. (c) Numerical (shaded areas) and analytical (dashed curve) results of Floquet quasi-energies ε_j versus lattice modulation.

oscillates between positive and negative values as the modulation parameter A/K along the z direction varies. In particular, the coefficient $\bar{C}$ approaches zero at certain points, which corresponds to the CDT condition under which inhibition of light tunneling occurs. Near these zero-coupling points, discrete diffraction of light due to waveguide coupling is dramatically suppressed [5,9], providing a new way for distortion-free image transmission. Furthermore, $\bar{C}$ can become negative at some increased modulations, which could lead to reversal of bandgap structures [15,16]. It is in these negative-coupling regimes that we expect to see anomalous diffraction and negative refraction associated with band reversal within the first Brillouin zone [15–18].

Our experimental approach for generation of 3D photonic lattices in a biased SBN crystal is illustrated in Fig. 2, where the 3D lattice-inducing beam is composed by superposition of two mutually incoherent lattice beams—one has decreasing intensity from input to output facets of the crystal, while the other has increasing intensity. Because of the need to match the waveguide coupling length [5,9], our induced lattice (30 μm transverse lattice spacing) has only a half modulation period along the z direction, as limited by the 2-cm-long crystal, yet it is enough for observing the predicated phenomena as a proof of principle. By adjusting the imaging plane of the amplitude mask and spatial coherence of the lattice-inducing beam, the intensity gradient along the z direction for each lattice beam is changed individually. Therefore, the induced structure can be "fine-tuned" by varying the intensity gradients of the two lattice-inducing beams while keeping the total beam intensity in the middle of the crystal essentially unchanged. Figure 2(b) shows a few typical snapshots of the lattice pattern taken at different transverse planes of the crystal.

We first perform a numerical simulation parallel to our experimental work by solving Eq. (1) with the beam propagation method (BPM). The BPM simulation results for a focused Gaussian probe beam propagating through the 3D photonic lattice at different z modulations are displayed in Figs. 3(a1)–(a3), where the normalized parameters used in simulation are $\Lambda = 8$, $K = 0.084$, and $z = 80$. Indeed, as expected from the theory, propagation

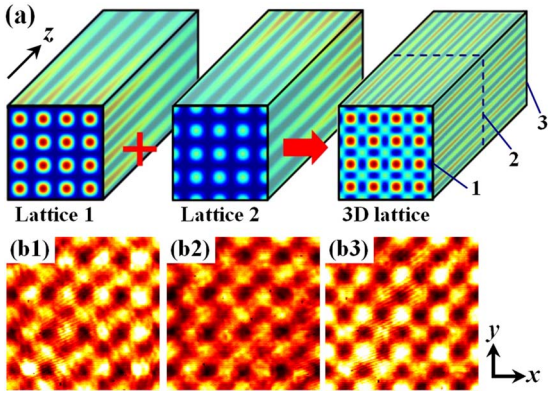

Fig. 2. (Color online) (a) Schematic of optical induction of 3D lattices in a biased nonlinear crystal by superposition of two lattice beams with opposite intensity gradients along z; (b) experimental results of transverse patterns taken at the three different z positions marked in the right panel of (a), corresponding to input, middle, and output facets of the crystal.

of the probe beam is strongly affected by the z modulation. At $A = 0$ (corresponding to a 2D lattice, i.e., no z modulation), the probe beam exhibits strong discrete diffraction, but such diffraction is completely suppressed at $A = 0.4$ (corresponding to the CDT condition). In Fig. 3(a4), we show typical beam propagation along the z direction obtained under the CDT condition $A = 0.4$. However, coupling-induced diffraction comes back with further increase of the z modulation to $A = 1.0$ [Fig. 3(a3)]. Our corresponding experimental results are shown in Figs. 3(b1)–(b3), obtained by sending a circular Gaussian beam into the 3D lattice established in Fig. 2. In agreement with the simulation, the first order of CDT is observed at $A = 0.4$, but discrete diffraction occurs again at further increased z modulation. In fact, as the modulation is increased even further, we found that higher-order CDT also takes place due to the oscillation of the coupling coefficient shown in Fig. 1(c). Specifically, the second-order CDT occurs at $A = 1.6$, and then it is destroyed again by strong coupling at $A = 2.0$.

Next, we demonstrate the principle of image transmission at the CDT condition. To do so, we simply launch an input image of a "+" pattern into the lattice structure and examine the output at different levels of z modulation. The simulation and experimental results are shown in Figs. 3(c) and 3(d), respectively. In the 2D lattice ($A = 0$), the input image is strongly distorted after propagating through the lattice. However, in the 3D photonic lattice under the CDT condition ($A = 0.4$), the input image maintains its shape after linear propagation without severe distortion. As expected, further increase of z modulation leads to image distortion again.

Finally, we demonstrate anomalous diffraction and negative refraction in the negative-coupling regime.

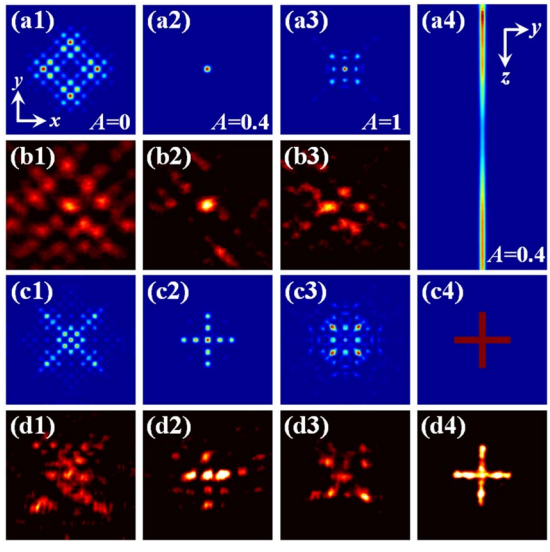

Fig. 3. (Color online) (a), (c) Numerical and (b), (d) experimental demonstrations of (a), (b) CDT and (c), (d) image transmission. (a1)–(a3) and (b1)–(b3) show output transverse patterns of a focused Gaussian probe beam at different modulations, and (a4) shows a side view of the probe beam propagating along z under the CDT condition $A = 0.4$. (c1)–(c3) and (d1)–(d3) show corresponding output patterns of a "+" shape [input shown in (c4) and (d4)] after propagating through the 3D lattice.

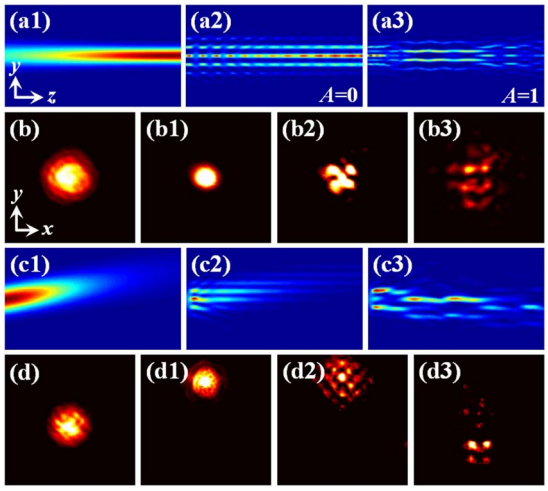

Fig. 4. (Color online) (a), (c) Numerical and (b), (d) experimental results of (a), (b) beam diffraction and (c), (d) refraction under different conditions. (a1)–(a3) and (c1)–(c3) show side views of a probe beam propagating when no lattice, a 2D lattice ($A = 0$), or a 3D lattice ($A = 1.0$) is present, respectively. (b1)–(b3) and (d1)–(d3) show output transverse patterns of a probe beam [input shown in (b) and (d)] taken from the experiment under different conditions corresponding to (a), (c). (a), (b) For diffraction, the beam is launched straight along z direction but is initially focused at the crystal output. (c), (d) For refraction, the beam is initially tilted upward relative to the z direction.

According to our theoretical analyses and numerical simulations, when $0.4 < A < 1.6$, the index modulation of the 3D lattice leads to a negative effective coupling coefficient. We thus take $A = 1.0$ as an example. Results for the diffraction/refraction management under this condition from BPM simulation and experiments are displayed in Fig. 4. To visualize the anomalous diffraction under the linear condition [18], a focused Gaussian beam is launched and monitored while propagating through the crystal [Figs. 4(a) and 4(b)]. For the experiment of negative refraction, the Gaussian beam is titled upward at the half of the first-order Bragg angle of the 2D lattice ($A = 0$) [Figs. 4(c) and 4(d)]. Obviously, in the 2D lattice (i.e., $A = 0$, no modulation), the beam undergoes normal diffraction and refraction, as it does in a homogenous medium. However, when the effective coupling coefficient is negative (e.g., $A = 1.0$), the initially focused Gaussian beam diverges, and the initially upward-tilted beam bends downward, exhibiting typical behavior of anomalous diffraction and negative refraction [17–19]. These experimental observations agree well with our theoretical results. Note that the negative refraction observed here does not require the two-beam excitation technique, reflecting to a rather different mechanism [18,19].

In summary, we have optically induced 3D photonic structures and demonstrated novel phenomena, including two-dimensional light tunneling inhibition and CDT-based image transmission, as well as anomalous diffraction and negative refraction originating purely from the flipping of bandgap structures.

This work was supported by the National Science Foundation (NSF), the U.S. Air Force Office of Scientific Research (USAFOSR), and the 973 program. We thank A. Szameit and Y. V. Kartashov for discussions.

References

1. D. N. Christodoulides, F. Lederer, and Y. Silberberg, Nature **424**, 817 (2003).
2. F. Lederer, G. I. Stegeman, D. N. Christodoulides, G. Assanto, M. Segev, and Y. Silberberg, Phys. Rep. **463**, 1 (2008).
3. H. S. Eisenberg, Y. S. Silberberg, R. Morandotti, and J. S. Aitchison, Phys. Rev. Lett. **85**, 1863 (2000).
4. S. Longhi, M. Marangoni, M. Lobino, R. Ramponi, P. Laporta, E. Cianci, and V. Foglietti, Phys. Rev. Lett. **96**, 243901 (2006).
5. A. Szameit, Y. V. Kartashov, F. Dreisow, M. Heinrich, T. Pertsch, S. Nolte, A. Tünnermann, V. A. Vysloukh, F. Lederer, and L. Torner, Phys. Rev. Lett. **102**, 153901 (2009).
6. A. Szameit, I. L. Garanovich, M. Heinrich, A. A. Sukhorukov, F. Dreisow, T. Pertsch, S. Nolte, A. Tünnermann, and Y. S. Kivshar, Nature Phys. **5**, 271 (2009).
7. K. Shandarova, C. E. Rüter, D. Kip, K. G. Makris, D. N. Christodoulides, O. Peleg, and M. Segev, Phys. Rev. Lett. **102**, 123905 (2009).
8. N. K. Efremidis, P. Zhang, Z. Chen, D. N. Christodoulides, C. E. Rüter, and D. Kip, Phys. Rev. A **81**, 053817 (2010).
9. Y. V. Kartashov, A. Szameit, V. A. Vysloukh, and L. Torner, Opt. Lett. **34**, 2906 (2009).
10. P. G. Kevrekidis, J. Gagnon, D. J. Frantzeskakis, and B. A. Malomed, Phys. Rev. E **75**, 016607 (2007).
11. K. Staliunas and R. Herrero, Phys. Rev. E **73**, 016601 (2006).
12. P. Zhang, R. Egger, and Z. Chen, Opt. Express **17**, 13151 (2009).
13. J. Xavier, P. Rose, B. Terhalle, J. Joseph, and C. Denz, Opt. Lett. **34**, 2625 (2009).
14. C. E. Creffield, Phys. Rev. B **67**, 165301 (2003).
15. A. Locatelli, M. Conforti, D. Modotto, and C. De Angelis, Opt. Lett. **30**, 2894 (2005).
16. A. Locatelli, M. Conforti, D. Modotto, and C. De Angelis, Opt. Lett. **31**, 1343 (2006).
17. T. Pertsch, T. Zentgraf, U. Peschel, A. Bräuer, and F. Lederer, Phys. Rev. Lett. **88**, 093901 (2002).
18. P. Zhang, C. Lou, S. Liu, J. Zhao, J. Xu, and Z. Chen, Opt. Lett. **35**, 892 (2010).
19. C. R. Rosberg, D. N. Neshev, A. A. Sukhorukov, Y. S. Kivshar, and W. Krolikowski, Opt. Lett. **30**, 2293 (2005).